

Magmatically Triggered Slow Slip at Kilauea Volcano, Hawaii

Benjamin A. Brooks,¹ James Foster,¹ David Sandwell,² Cecily J. Wolfe,¹ Paul Okubo,³ Michael Poland,³ David Myer²

The discovery, primarily at subduction zones, of spontaneous aseismic slip events (slow slip events, SSEs) has led to the recognition that SSEs represent behavior between steady sliding and dynamic earthquake rupture. Furthermore, slow slip, down dip of plate boundary seismicity (30- to 45-km depth), may delineate the lower boundary of the locked plate interface and constrain the fault geometry of great magnitude (M) 8 to 9 earthquakes (I). SSEs have also been found recently at depths shallower than ~ 10 km on the decollement (or related faults) underlying the mobile south flank of Hawaii's Kilauea volcano (2, 3). The Kilauea SSEs occur in a

different tectonic setting and rheological context: up dip of the region of decollement seismicity, although potentially within the locked portion that can rupture in earthquakes greater than $M7$ (4, 5). Within a rate-state-dependent friction theoretical context, SSEs are believed to occur at the transition between unstable and stable sliding. A general understanding, however, of SSE initiation is still unresolved. We show that a dike intrusion in June 2007 triggered an SSE at Kilauea.

During 17 to 19 June 2007, Kilauea was intruded by a dike that originated from the volcano's summit and extended its east rift zone (ERZ) by as much as ~ 1 m (6). We created an interferogram from two Ad-

vanced Land Observing Satellite synthetic aperture radar images to produce a high-resolution map of the intrusion (Fig. 1A). The interferogram indicates subsidence at Kilauea's summit and two uplift lobes (separated by a narrow subsidence zone) related to the dike intrusion. Continuous Global Positioning System (GPS) data further revealed anomalous, southeast-directed, centimeter-scale horizontal motions at sites far from the dike (stations PGF1, 5, and 6 in Fig. 1 and fig. S1, A to D) that cannot be explained by models of the dike intrusion and are best explained as arising from an SSE. Horizontal motions from the four previous SSEs are nearly identical, although the 17 June event has a larger magnitude (Fig. 1A) (2, 3). Additionally, south flank coastal sites exhibit subsidence not predicted by the dike model, although similar to the vertical motion during prior SSEs (fig. S1E). Lastly, ~ 24 hours after dike-related seismicity started, seismicity increased abruptly in the north-south trending region that previously displayed SSE-triggered seismicity (2, 3) (Fig. 1A). Although this region has experienced past elevated seismicity unassociated with SSEs, it was quiescent during previous ERZ dike intrusions in 1997 and 1999; thus, elevated activity during the 2007 event is consistent with SSE occurrence.

Hourly GPS positions show that SSE-related motions likely began ~ 15 to 20 hours after the intrusion, suggesting that the intrusion triggered the SSE (Fig. 1B). We further test this hypothesis by modeling stress changes in the south flank due to secular deformation and the intrusion (Fig. 1C). The models imply that the intrusion increased the Coulomb failure stress on shallowly landward-dipping fault planes (the presumed geometry of the SSE slip surfaces) by roughly the same amount as secular deformation since the last SSE [deep rift opening combined with decollement creep (4)]. These results, in concert with the observation that no previous SSEs were directly preceded by intrusions but rather occurred during times of normal background deformation, suggest that both extrinsic (intrusion-triggering) and intrinsic (secular fault creep) fault processes produce SSEs at Kilauea.

References and Notes

- S. Y. Schwartz, J. M. Rokosky, *Rev. Geophys.* **45**, 10.1029/2006RG000208 (2007).
- B. A. Brooks, J. H. Foster, M. F. Bevis, C. J. Wolfe, M. Behn, *Earth Planet. Sci. Lett.* **246**, 207 (2006).
- P. Segall, E. K. Desmarais, D. Shelly, A. Miklius, P. Cervelli, *Nature* **442**, 71 (2006).
- V. Cayol, J. H. Dieterich, A. T. Okamura, A. Miklius, *Science* **288**, 2343 (2000).
- S. Owen, R. Burgmann, *J. Volcanol. Geotherm. Res.* **150**, 163 (2006).
- M. Poland et al., *EOS Trans. Am. Geophys. Union* **89**, 37 (2008).
- We thank A. Miklius, K. Kamibayashi, M. Sako, and P. Segall for their collaboration on operation of the Kilauea GPS network.

This work was supported by NSF's Geophysics program.

Supporting Online Material

www.sciencemag.org/cgi/content/full/321/5893/1177/DC1

Materials and Methods

Fig. S1

References

11 April 2008; accepted 10 June 2008

10.1126/science.1159007

¹School of Ocean and Earth Science and Technology, University of Hawaii, 1680 East-West Road, Honolulu, HI 96822, USA.

²Scripps Institution of Oceanography, La Jolla, CA 92093-0225, USA. ³Hawaiian Volcano Observatory, U.S. Geological Survey, Hawaii National Park, HI 96718, USA.

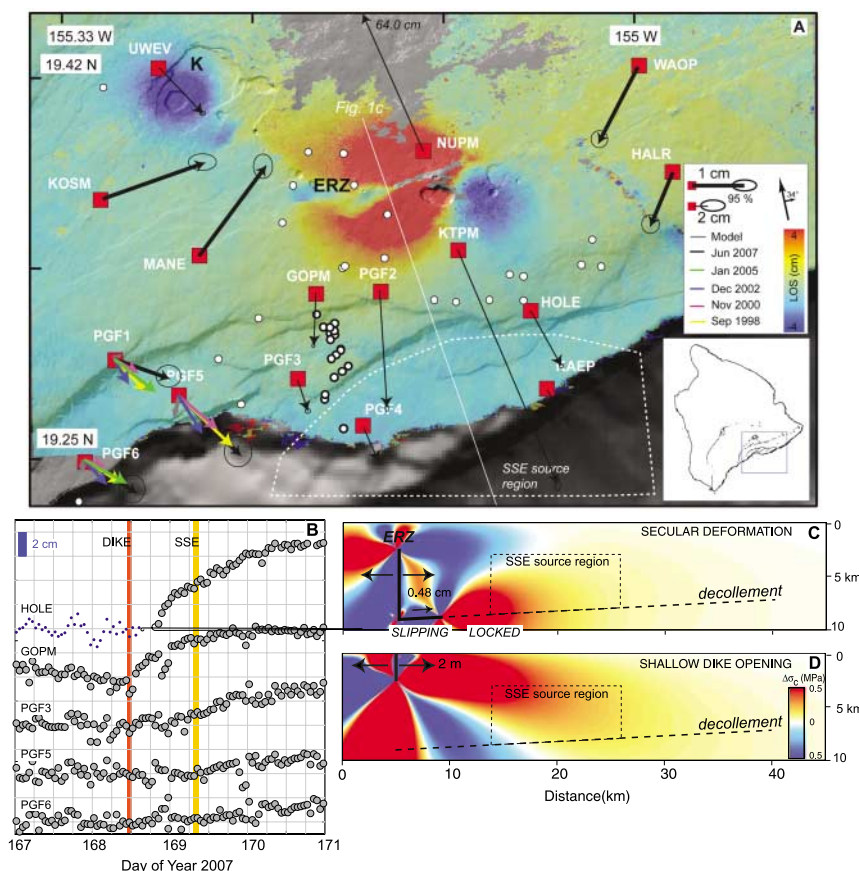


Fig. 1. (A) Line-of-sight interferometric displacement map from ALOS PALSAR (Phased Array Type L-Band Synthetic Aperture Radar) ascending acquisitions in fine beam dual polarization mode (FBD-HH, 14 MHz) on 5 May and 20 June 2007. K, Kilauea summit caldera; ERZ, east rift zone. Black vectors with arrows show static GPS horizontal displacements estimated from times around the dike intrusion event. Because of large dike-related displacements, sites are plotted with two different scales. Other colored vectors at sites PGF1, 5, and 6 show horizontal displacements from previous SSEs; gray vectors show expected displacements due to the dike intrusion (see also fig. S1). White circles show earthquake epicenters (from U.S. Geological Survey Hawaii Volcano Observatory catalog) ± 5 days from 17 June for all events between depths of 5 to 10 km. White circles with thicker outline indicate north-south band of events that occurred 24 hours after the dike intrusion started. (B) GPS position (projected onto average motion direction) time series for selected sites. Approximate timing of dike initiation and SSE initiation indicated with vertical colored bars. Coulomb failure stress models for (C) secular deformation and (D) shallow dike opening scenarios.